Domain Adaptations for Guided Wave SHM of Composites: Towards Fleet Monitoring

Sebastiaan van Baars Buisman[1], Gabriel Michau[2], René Alderliesten[3] and Olga Fink[4]

[1,2,4] *ETH Zurich, Swiss Federal Institute of Technology, Zurich, Switzerland*

[1,3] *TU Delft, Delft, Netherlands*

ABSTRACT

Different operating conditions can hinder the capability of data-driven models to make predictions regarding the components remaining life. In this paper, domain adaptation (DA) with deep learning is introduced as a potential method to align features from data collected under dissimilar conditions. The work focuses on DA applied to the classification of the remaining useful properties for components in dissimilar boundary conditions. The proposed approach was evaluated on three carbon fibre reinforced polymer coupons with a notch. The dataset was collected by sensing the damage state with guided waves with a sequential alteration of the boundary conditions during the experiment. The main application of this work is thus the transferability of guided wave datasets collected under different boundary conditions. An exemplar case could be different structural components of a wing.

Taking into consideration the pairwise correspondence of few samples in both domains, a Neural Network (NN) architecture called Feature Alignment Neural Network (FANN) is introduced with a novel loss function. The loss was inspired by multi-dimensional scaling (MDS) and the overlap of pairwise corresponding points. To simulate the unsupervised nature of the target domain, only limited data points were used for the pairwise correspondence objective. The FANN was used to learn a new feature space used as input to a classifier. The results show that the FANN can learn a robust overlap function for both domains, and that when used in combination with Adaptive Batch normalisation (AdaBn) in the classifier, the model becomes capable of making reliable predictions in both domains.

1. INTRODUCTION

Damage due to fatigue affects the operational availability of aircraft. Structural health monitoring (SHM) research focuses on condition based maintenance (CBM) to predict the damage in real-time. The objective of CBM is, thus, to replace parts only when truly necessary. The procedure has the potential to decrease the amount of maintenance checks and increase the operational availability, thus, becoming more cost-efficient.

Aircraft however consist of hundreds of dissimilar structural components. When structural health monitoring methods are implemented, it would require that all these dissimilarities are taken into account. Current SHM research, typically, takes advantage of a consistent lab setup to run a series of experiments and develop a model (see Figure 1). This, however, will inevitably lead to implementation issues when the same model is tested on structural components with dissimilar conditions. For this reason, there is an urgency to start working on how current lab results can be implemented in aircraft towards monitoring the entire structure. One potential approach to solve this problem is to have a single model which can make predictions for dissimilar conditions (Gardner, Liu, & Worden, 2020). The advantage of this approach lies in the fact that it would not require a unique model to be developed for all individual components. An emerging technology that can achieve such a singular model is through domain adaptation (Kouw & Loog, 2018; M. Wang & Deng, 2018; Q. Wang, Michau, & Fink, 2020). Domain adaptation has recently gained attention due to the ability to solve problems on datasets originating from different distributions (Ajakan, Germain, Larochelle, Laviolette, & Marchand, 2014; X. Li, Zhang, Ding, & Sun, 2019; Bousmalis, Trigeorgis, Silberman, Krishnan, & Erhan, 2016; Pan, Tsang, Kwok, & Yang, 2011).

As an example of the dissimilar conditions, different boundary conditions are studied in this research. For a structural component, the boundary condition is the way the

Figure 1. A typical lab setup for a CFRP fatigue tested coupon (prognostics group, 2020). Such a component could be used in e.g. a wing part

material is held at its extremities. A visualisation of both clamped and traction free boundary conditions (BCs) is presented in Figure 2. A model trained as such could make diagnostics predictions regardless of which of the two BCs it is held in. If effective, this approach could limit the total number of models needed to monitor a full aircraft and improve the transferability of the models.
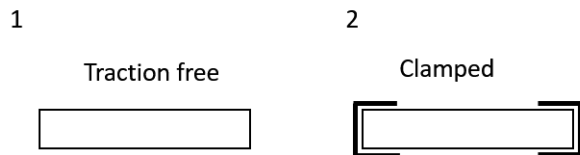

Figure 2. An overview of the relevant boundary conditions for the proposed experiment.

In this paper, guided waves, a prominent SHM technology is used to make diagnostics models taking into account the different BCs. Guided wave technology uses a series of sensors and actuators to send and receive lamb wave signals (Mitra & Gopalakrishnan, 2016). The alteration of boundary conditions causes a domain shift, hindering the diagnostics capability of current models.

The model itself is developed to monitor damage growth for three carbon fibre reinforced polymer (CFRP) coupons from the NASA prognostics repository with layup $[0_2/90_4]_S$ (prognostics group, 2020). CFRPs have outstanding po-

tential to lower the weight of aircraft structures and have superb material properties. The fatigue and degradation phenomena of CFRPs is however highly unpredictable (Eleftheroglou, Zarouchas, Loutas, Alderliesten, & Benedictus, 2018). One key property which is well correlated to the Remaining Useful Life (RUL) is the delamination growth (Saxena et al., 2011). Predicting the area of the delamination can give direct insight into the current repair requirements. Given this reason, the model developed is trained to predict the delamination size.

Based on the above points, the research question is formulated as follows: "Can domain adaptation be used to transfer data with dissimilar boundary conditions such that the delamination can be predicted accurately for both clamped and traction free data?"

The rest of this paper is structured as follows: Chapter 2 outlines how the dataset is acquired, Chapter 3 describes the Damage Indicator extraction approach and the proposed framework for this problem, Chapter 4 describes the experimental results, Chapter 5 is a discussion on the presented result and Chapter 6 contains concluding remarks.

2. DATA ACQUISITION

The three CFRP coupons with a notch have been subjected to a tension-tension fatigue test with a frequency of 5 Hz and stress ratio $R \approx 0.14$ until failure[1]. Periodically, the fatigue test is interrupted to collect data. To do so, a series of actuators emit signals which travel through the material in the form of lamb waves (Chiachio, Chiachio, Saxena, & Goebel, 2013). Subsequently, a group of sensors collect the signals. The change of the signal as the fatigue test proceeds contains damage fingerprints which can quantify damage growth. Each time data is collected is referred to as an SHM cycle from here onward[2]. In order to quantify the delamination area, four signals have been selected as presented in Figure 3. Due to the delamination starting at the notch, these signals consistently travel through the delamination region. The selected frequency for this experiment is 150 KHz. It is the lowest frequency available and has been selected due to its more pronounced sensitivity to large damage compared to the higher frequency signals (Shoja, Berbyuk, & Boström, 2018). Furthermore, as the test is paused, an X-ray visualisation is made of the coupon. The X-ray visualisations are used to develop ground truth labels of the delamination area.

During the fatigue test interruptions, the boundary condi-

---

[1]This experiment can be performed with less coupons but the performance might be impacted.
[2]An SHM cycle is not be confused with a fatigue cycle. A single SHM cycle is typically performed after various fatigue cycles.

tion of the coupon is sequentially altered. This is done by altering the way the coupon is held during data acquisition. This process is performed for clamped and traction free boundary conditions. As the boundary conditions are altered, however, the damage due to fatigue remains the same. The different boundary conditions will cause the stress levels in the material to be different. Consequently, the lamb wave propagation is also altered, causing small changes to the sensed signals. These altered conditions will be used to setup the domain adaptation task.
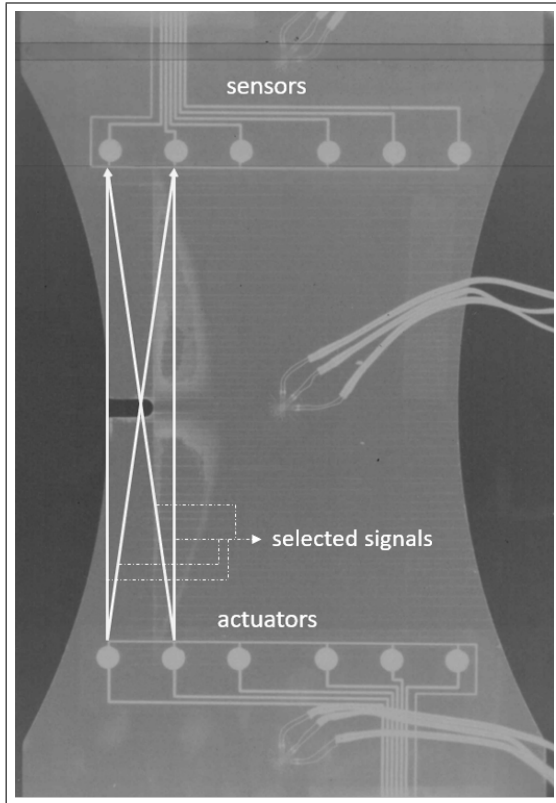

Figure 3. X-ray visualisation of coupon $L1\_S11\_F$. The four arrows present the paths selected (prognostics group, 2020).

3. METHOD

The proposed framework comprises five steps:

1. Damage Indicators (DIs) are extracted from a group of selected signals.

2. The FANN architecture is trained to align the indicators of dissimilar BC's.

3. A classifier is trained with the aligned source features (BC 1) and tested with the aligned target features (BC 2).

4. To show the added value of the FANN alignment, the result is compared to training the classifier on the raw Damage Indicators without alignment. This task will be referred to as the Baseline from here onward. It will show whether the domain adaptation task is solvable without any additional network design.

5. Adaptive Batch Normalisation (AdaBn) (Y. Li, Wang, Shi, Liu, & Hou, 2019) is integrated in both developed methodologies.

A full overview of the proposed framework is presented in Figure 4. The individual steps are elaborated in more detail in the following Sections.

3.1. Damage Indicator extraction

A feature engineering approach is adopted in order to extract relevant information from the signals. Inspired by (Xu, Yuan, Chen, & Ren, 2019), a vector of six Damage Indicators is extracted. Damage Indicators compare the signal of the damaged material to the original signal before any damage accumulation. It is a comparative measure typically ranging from $0 \rightarrow 1$. The extracted indicators are: cross-correlation, spatial phase difference, spectrum loss, central spectrum loss, differential curve energy and normalised correlation moment. They are a combined selection of both frequency and time domain indicators. A full list of the mathematical indicator extraction algorithms is presented in Table 1. The indicators are joined together into a single vector to serve as damage fingerprints to predict the delamination.

3.2. Stage 1: Feature Alignment Neural Network

In this paper, a FANN architecture is proposed to adapt features from two dissimilar boundary conditions: clamped and traction free. The FANN has an input size of 6 units and consists of 3 dense layers, each with 6 units. The input of the FANN are the extracted indicators from the clamped and traction free data. The architecture uses weight sharing for both input vectors. The FANN learns a new latent feature space which is subsequently used as input to a classifier to predict the delamination.

The properties that the generated latent space must satisfy are twofold. Firstly, it must overlap the data points from both domains that were measured at the same fatigue level. Secondly, it must maintain the relationship between damaged and undamaged data. To do so, the inter-point distance of the learned latent features must remain the same for each domain. Thus the FANN is trained with two losses $\mathcal{L}_P$ and $\mathcal{L}_{mds}$.

The first loss, $\mathcal{L}_P$, minimises the distance of the pairwise corresponding vectors in the clamped and traction free domains:

$$\mathcal{L}_P = \frac{1}{|S|} \sum_{i \in S, j \in T} (X_i - X_j)^2$$

Table 1. Damage indicators used for extraction from the selected signals. The baseline and the damaged signals are presented by B and D respectively, $b(t_n)$ and $d(t_n)$ present the magnitude of B and D signal at a specified time t_n and w presents the frequency spectrum of the signal.

Damage Indicator	mathematical extraction algorithm
Cross correlation	$DI = 1 - \sqrt{\dfrac{\left[\int_{t_1}^{t_2} B(t)D(t)\mathrm{d}t\right]^2}{\int_{t_1}^{t_2} B^2(t)\mathrm{d}t \int_{t_1}^{t_2} D^2(t)\mathrm{d}t}}$
Spatial phase difference	$DI = \int_{t_1}^{t_2}(\tilde{D}(t) - \alpha B(t))^2 \, \mathrm{d}t, \tilde{D}(t) = \dfrac{D(t)}{\sqrt{\int_{t_1}^{t_2} D^2(t)\mathrm{d}t}}, \alpha = \dfrac{\int_{t_1}^{t_2} D(t)B(t)\mathrm{d}t}{\int_{t_1}^{t_2} B^2(t)\mathrm{d}t}$
Spectrum loss	$DI = \dfrac{\int_{\omega_1}^{\omega_N} |B(\omega)-D(\omega)|\mathrm{d}\omega}{\int_{a'}^{a_N} |B(\omega)|\mathrm{d}\omega}$
Central spectrum loss	$DI = \dfrac{a(\omega)-b(\omega)}{a(\omega)}, a(\omega) = \max(B(\omega)), b(\omega) = \max(D(\omega))$
Differential curve energy	$DI = \dfrac{\sum_{n=2}^{N}[b(t_n)-b(t_{n-1})]^2}{\sum_{n=2}^{N}[B(t_n)-B(t_{n-1})]^2}, b(n) = B(n) - D(n)$
Normalized Correlation Moment	$DI = \dfrac{\int_{\tau=t_1}^{\tau=t_2} \tau^k |r_{HH}(\tau)|\mathrm{d}\tau - \int_{\tau=t_1}^{\tau=t_2} \tau^k |r_{HD}(\tau)|\mathrm{d}\tau}{\int_{\tau=t_1}^{\tau=t_2} \tau^k |r_{HH}(\tau)|\mathrm{d}\tau}, r_{HD}(\tau) =$ $\int_{-\infty}^{+\infty} B(t)D(t-\tau)\mathrm{d}t, r_{HH}(\tau) = \int_{-\infty}^{+\infty} B(t)B(t-\tau)\mathrm{d}t$

where S is the source domain and T is the target domain.

The second component in the loss function is inspired by the concept of multidimensional scaling (Michau & Fink, 2021):

$$\mathcal{L}_{mds} = \sum_S \frac{1}{|S|} \sum_{(i,j)\in S} \left|\|\|X_i-X_j\|_2 - \widehat{\eta}_S\| F_i-F_j \|_2\|_2\right|, \tag{1}$$

where

$$\forall S \in \left\{ \ \text{Source} \ \right\}, \quad \widehat{\eta}_S = \text{Argmin}_{\tilde{\eta}_S} \mathcal{L}_{mds}(\tilde{\eta}_S) \tag{2}$$

This loss function compares the Euclidian distance of vectors in both, the input DI space and the latent feature space. The objective is to ensure that these distances remain the same given the scaling factor $\widehat{\eta}_S$. In other words, the objective is to keep the inter-point distance of the input space and latent space proportional. Consequently, the relationship between damaged and undamaged data is kept.

Bringing together both loss functions, the loss of the FANN is presented as follows:

$$\mathcal{L}_{FANN} = \mathcal{L}_p + \mathcal{L}_{mds} \tag{3}$$

The FANN architecture is trained with an Adam optimiser with the learning rate $l = 1e^{-4}$, $\beta_1 = 0.9$ & $\beta_2 = 0.999$. It consists of Dense layers as follows: $\{6, 6, 6\}$. The batch size is 100, and the model is trained for 600 epochs which is found to converge the objective function. These parameters were determined through a grid search.

3.3. FANN Data Selection Methodology

The developed model must be able to monitor the degradation trajectory of unique components from as early in their lifetime as possible. In such cases, data only from the early life of the target can be used for the training (Michau, 2019). In doing so, a semi-supervised simulation scenario is provided. Thereby, the complete run-to-failure training phase can be performed in e.g. a laboratory test setting, and the results can be transferred to an in-aircraft structural component. In order to design a model in agreement with this objective, the pairwise correspondence loss is only optimised with pairs before substantial damage accumulation. By only aligning these points, the individual component fatigue state can be monitored as it develops from an early stage. This constraint is effectively implemented by aligning the points of the first 10 cycles only.

An overview of the FANN architecture is presented in Figure 4 as Stage 1. In the figure, it can be observed that the MDS loss is only applied to the source domain. This is selected to align the study with existing cases where, typically, full knowledge of the source domain is available.

3.4. Stage 2: Classification

Even though damage growth is continuous, it was decided not to define the task as a regression problem but rather as a classification problem with 5 classes. By setting up the problem as a classification task, robust maintenance decisions can be made as the classes only present
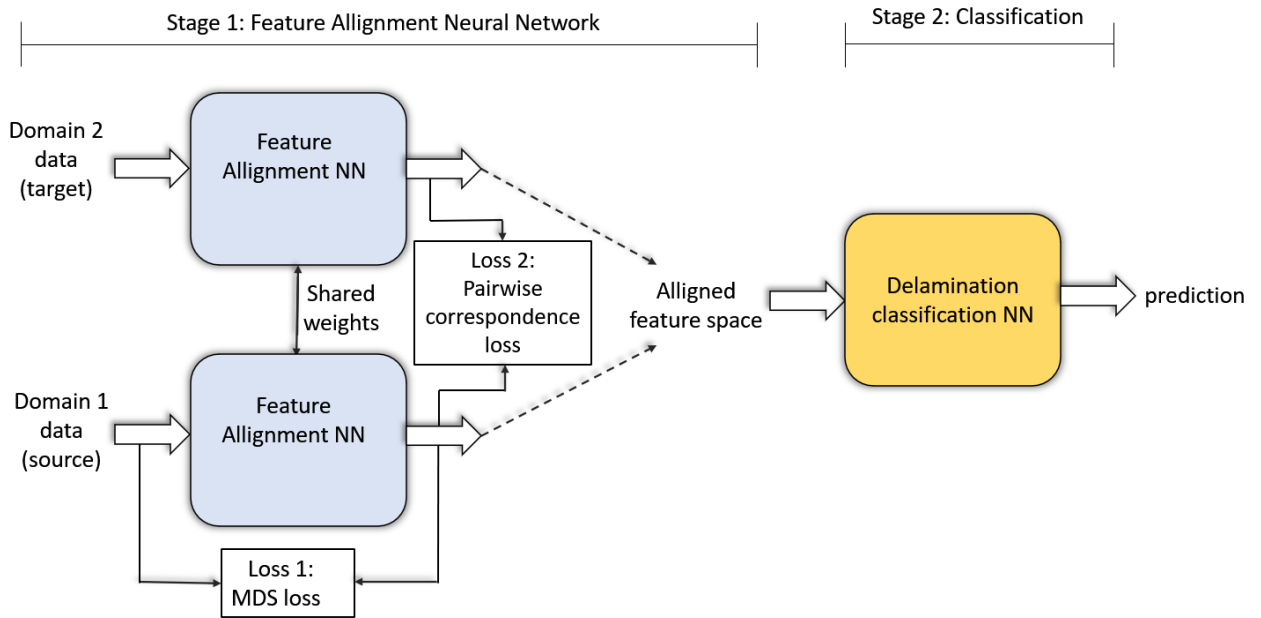
Figure 4. Visualisation of the full framework. The gradients are not propagated between the two stages.

coarse changes in the continuous damage growth. The training samples were distributed equally into 5 classes. The number of classes is selected based on expert advice such that the damage can be calculated precisely while not being too sensitive to noise (Ewald, Groves, & Benedictus, 2019). In doing so, an aircraft operator could select its maintenance requirements as e.g. level 2 and can monitor the damage after each flight cycle until the specified level is reached.

As mentioned in the previous Section, the learnt latent feature space of the FANN is of the same size as the input DI space. To make the delamination prediction, the learnt latent features are used as input to a classifier neural network (NN).

The classification NN is designed with 24 inputs. These inputs correspond to the appended features of all four selected signals at a single time step. The architecture is designed through a grid search approach. The network architecture consists of Dense layers as follows: $\{24, 24, 24, 5\}$. Leaky Relu activation is used with $\alpha = 0.2$ in the first three layers. The final layer used a Softmax activation and a Categorical Cross Entropy loss function. All layers used the "He initialisation" (He, 2014). Lastly, an Adam optimiser is used with the initial learning rate $l = 0.001$.

The entire framework, including both the FANN and the classifier is presented in Figure 4.

3.5. Adaptive Batch Normalisation

Adaptive batch normalisation is inspired by batch normalisation. Batch normalisation (BN) layers are used to mitigate the side effects of a covariate shift. To do so, a BN normalises a feature space x_i of dimension k as follows:

$$\tilde{x}_i = \frac{x_i - \mathbb{E}\left[x_{.i}\right]}{\sqrt{\text{Var}\left[x_{.i}\right] + \xi}}$$
$$y_i = \gamma_i \tilde{x}_i + \beta_i \tag{4}$$

Where $i \in \{1...k\}$, γ_i and β_i are trainable parameters, y_i is the output and ξ presents a small value for numerical stability. By using BN, the input of a subsequent layer is normalised and the distribution of values remains unchanged. AdaBn assumes that the distribution differences of individual layers causes the performance decrease on the target domain. It uses the same mechanism as BN but fine-tunes the statistical parameters using data of the target domain.

4. EXPERIMENTAL RESULTS

The alignment of the FANN for both boundary conditions must be analysed. To do so, input features of both domains are passed through the FANN. A principal component analysis (PCA) is used to visualise the latent space. The first two principal components (PCs) of the aligned latent feature space are presented in Figure 5. The colour

coding presents the current SHM cycle. It can be noted that the domains of both visualisations are very similar. Individually, a handful of outliers can be seen, but considering that the full dataset consists of over 20000 vectors for each BC, the domain adaptation appears to be achieved well. The next step in the validation process is to make delamination predictions.

To compare the delamination prediction results, the developed methodology is compared to three other approaches. The first approach, as described earlier, uses the classifier on the raw Damage Indicators and is called the Baseline. The second approach uses the raw Damage Indicators & Baseline classifier with the addition of the Adaptive Batch Normalisation (AdaBn) layers and is inspired by (Y. Li et al., 2019). The AdaBn layer is most effective when applied to the first two layers of the Baseline architecture. Next, the learnt latent features from the FANN were tested as inputs to the same classifier. Lastly, the learned features were used as inputs to the classifier with the addition of Adaptive Batch Normalisation.

The delamination growth is a continuous process[3]. As a result, the impact an inaccurate prediction has is proportional to how far off it is from the correct class. To give an example, if a delamination of class 5 (corresponding to the largest area), is misclassified as a delamination of class 1, its impact on operational potential is much stronger than if it is classified into class 4. For this reason, an additional error metric is designed to take into account the magnitude of inaccurate predictions. The desired behaviour is compared to the confusion matrix where optimally, all values are as close as possible to the principal diagonal. For this reason, the novel metric is named *confusion deviation*. The metric scales quadratically based on how far away from the principle diagonal the prediction is in the confusion matrix. Mathematically, the new metric is determined as follows:

$$Conf.\ dev. = \sum_{i=0}^{m} \sum_{j=0}^{m} C \circ A \qquad (5)$$

Where $A_{i,j} = (i - j)^2$, C presents the confusion matrix, $\circ$ presents the element-wise product and m presents the number of classes to be classified.

The results of the experiments are presented as two one-to-one domain adaptation tasks. In the first task, the algorithms were trained with clamped data as the source and tested with traction free as the target. In the second task, the order is reversed. Due to the small volume of labelled data, the task is ran 10 times and the mean and standard deviation of all results are reported. The results

of these experiments are reported in Tables 2 & 3.

The results show that using the Baseline leads to a testing accuracy of approximately 76%. Adaptive Batch Normalisation has a positive effect on both domain adaptation tasks, but its improvement is limited by approximately 5%. Using the feature space learned by the FANN to train and test the classifier leads to a substantial accuracy drop of approximately 55% compared to the Baseline. The drop is explained by the unrestricted optimisation process of the FANN architecture. Since the only requirements used were the overlap of the pairwise correspondent points and the preservation of the inter-point distance, the loss is minimised when the latent space shrinks. Since the classification architecture is not altered in any way, this leads to a significant drop in accuracy. To solve this issue, the aligned features were used in combination with AdaBn in the classifier. This novel approach brings a further improvement of approximately 5% accuracy increase compared to the approach with AdaBn alone. Furthermore, the confusion deviation metric reaches a clear minimum in this setup. Thus, confirming the improvements for monitoring the structural health.

5. DISCUSSION

There are small differences in the solution quality of the two tasks. Observable is that training on traction free leads to slightly better mean results. This is likely due to the fact that the traction free domain is more stable and thus easier to train on. Further research is required to validate this statement.

Additionally, it is envisioned that the domain adaptation task must be reformulated as a regression problem in future work. This is because damage growth is continuous. It was however found to be challenging to setup due to the large absence of literature on domain adaptation for regression problems. The benefit of the classification setup is the applicability of the novel performance metric as well as the lower sensitivity to noise.

6. CONCLUSION

This paper proposes a framework based on domain adaptation for structural health monitoring to predict delaminations with dissimilar boundary conditions. The contribution of this work is the novel domain adaptation application for guided wave as well as the introduction of the FANN. The dataset was acquired by sequentially altering boundary conditions throughout the experiment. Thus, this work provides initial insights into the potential ways forward and presents potential challenges of applying domain adaptations to these datasets.

---

[3]see the Discussion section for a more elaborate statement as to why a regression setup was not used.

Table 2. Domain adaptation prediction results for clamped to traction free. The results of the FANN with the addition of AdaBn gives an improvement of nearly 10% over the baseline.

Clamped → Traction free	source		target	
	accuracy (%)	confusion deviation	accuracy (%)	confusion deviation
Baseline	93.2 ± 1.6	5.5 ± 1.5	75.9 ± 2.4	20.5 ± 2.5
AdaBn	94.7 ± 1.3	4.0 ± 1.0	78.3 ± 1.2	18 ± 1.0
FANN + Baseline	21.1 ± 0.4	105.2 ± 17.4	20.98 ± 0.4	105.7 ± 16.6
FANN + AdaBn	93 ± 1.5	4.9 ± 1.0	**84.50 ± 3.8**	**13 ± 4.0**

Table 3. Domain adaptation prediction results for traction free to clamped. The results of the FANN with the addition of AdaBn gives an improvement of nearly 10% over the baseline.

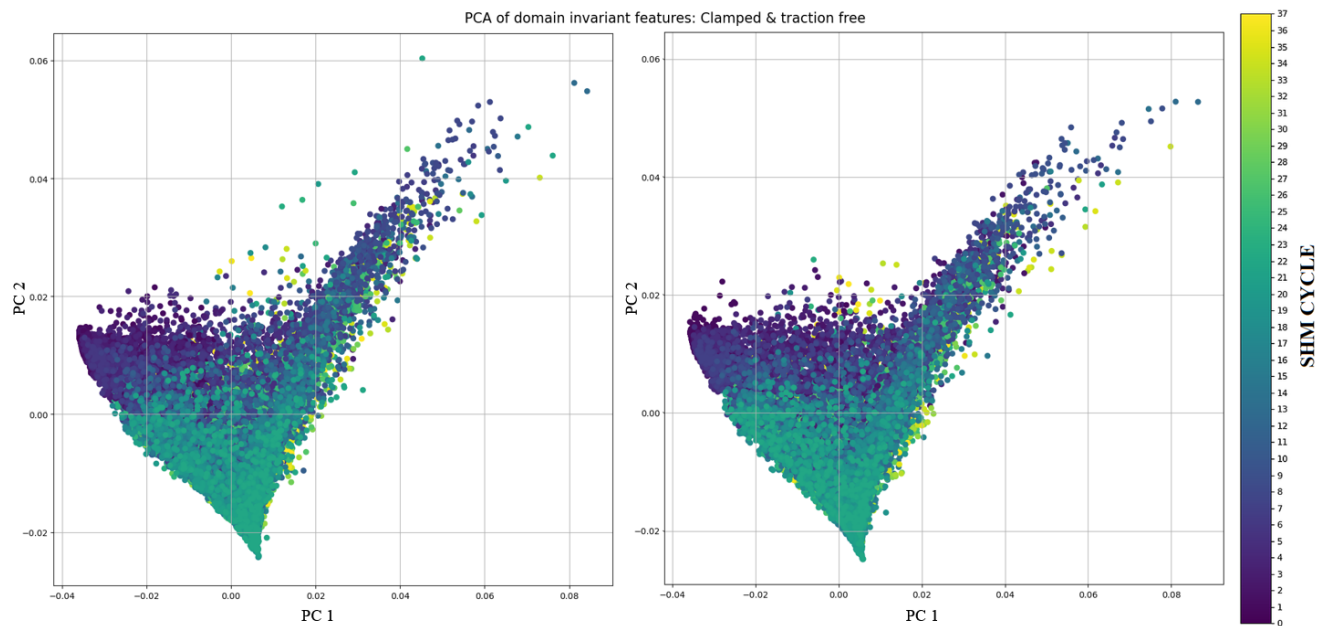| traction free → clamped	source		target	
	accuracy (%)	confusion deviation	accuracy (%)	confusion deviation
Baseline	93.4 ± 0.6	5.5 ± 0.5	76.0 ± 5.3	21.0 ± 7.0
AdaBn	91.6 ± 1.2	7.0 ± 1.0	80.6± 3.3	16.0 ± 2.0
FANN + Baseline	22.4 ± 3.8	113.1 ± 20.2	22.14 ± 4.1	112.5 ± 2.1
FANN + AdaBn	91.8 ± 2.8	5.9 ± 2.1	**85.71 ± 2.8**	**11.2 ± 2.2**

Figure 5. The left visualisation presents Clamped data and the right visualisation the Traction free data. The colour coding presents the current SHM cycle (A single SHM cycle consists of using the actuators and sensors to collect data and is typically done after various fatigue cycles). The pairwise correspondence loss was only trained with the first 10 fatigue cycles corresponding to SHM cycles $0 - 4$. The first two PCs of the aligned latent features are presented. These latent features are developed by passing the original Damage Indicators through the FANN. Both visualisations have aligned significantly in both shape and colour.

The results show that the developed methodology, which takes into consideration limited knowledge of the pairwise correspondence of both domains, and full knowledge of the source domain, improves the result of the domain adaptation classification task by at least 5% over the approach with AdaBn alone.

REFERENCES

Ajakan, H., Germain, P., Larochelle, H., Laviolette, F., & Marchand, M. (2014). Domain-Adversarial Neural Networks. (December).

Bousmalis, K., Trigeorgis, G., Silberman, N., Krishnan, D., & Erhan, D. (2016). Domain separation networks. *Adv. Neural Inf. Process. Syst.*(Nips), 343–351.

Chiachio, M., Chiachio, J., Saxena, A., & Goebel, K. (2013). Documentation for the fatigue dataset in composites. (September).

Eleftheroglou, N., Zarouchas, D., Loutas, T., Alderliesten, R., & Benedictus, R. (2018). Structural health monitoring data fusion for in-situ life prognosis of composite structures. *Reliab. Eng. Syst. Saf.*, *178*(April), 40–54. doi: 10.1016/j.ress.2018.04.031

Ewald, V., Groves, R. M., & Benedictus, R. (2019). DeepSHM: a deep learning approach for structural health monitoring based on guided Lamb wave technique. (March), 19. doi: 10.1117/12.2506794

Gardner, P., Liu, X., & Worden, K. (2020). On the application of domain adaptation in structural health monitoring. *Mech. Syst. Signal Process.*, *138*, 106550. doi: 10.1016/j.ymssp.2019.106550

He, K. (2014). Siraj Ali - Reference Questionnaire.pdf. *Proc. IEEE Int. Conf. Comput. Vis.*, 1026–1034.

Kouw, W. M., & Loog, M. (2018). Technical report: An introduction to domain adaptation and transfer learning. *arXiv*.

Li, X., Zhang, W., Ding, Q., & Sun, J. Q. (2019). Multi-Layer domain adaptation method for rolling bearing fault diagnosis. *Signal Processing*, *157*, 180–197. doi: 10.1016/j.sigpro.2018.12.005

Li, Y., Wang, N., Shi, J., Liu, J., & Hou, X. (2019). Revisiting batch normalization for practical domain adaptation. *5th Int. Conf. Learn. Represent. ICLR 2017 - Work. Track Proc.*, 1–12.

Michau, G. (2019). Domain adaptation for one-class classification: monitoring the health of critical systems under limited information.

Michau, G., & Fink, O. (2021). Unsupervised transfer learning for anomaly detection: Application to complementary operating condition transfer. *Knowledge-Based Syst.*, *216*, 106816. doi: 10.1016/j.knosys.2021.106816

Mitra, M., & Gopalakrishnan, S. (2016). Guided wave based structural health monitoring: A review. *Smart Mater. Struct.*, *25*(5). doi: 10.1088/0964-1726/25/5/053001

Pan, S. J., Tsang, I. W., Kwok, J. T., & Yang, Q. (2011). Domain adaptation via transfer component analysis. *IEEE Trans. Neural Networks*, *22*(2), 199–210. doi: 10.1109/TNN.2010.2091281

prognostics group, N. (2020). *Prognostics center of excellence (pcoe), prognostic-data-repository, composites data set.*

Saxena, A., Goebel, K., Larrosa, C. C., Janapati, V., Roy, S., & Chang, F. K. (2011). Accelerated aging experiments for prognostics of damage growth in composite materials. *Struct. Heal. Monit. 2011 Cond. Maint. Intell. Struct. - Proc. 8th Int. Work. Struct. Heal. Monit.*, *1*, 1283–1291.

Shoja, S., Berbyuk, V., & Boström, A. (2018). Delamination detection in composite laminates using low frequency guided waves: Numerical simulations. *Compos. Struct.*, *203*(July), 826–834. doi: 10.1016/j.compstruct.2018.07.025

Wang, M., & Deng, W. (2018). Deep Visual Domain Adaptation : A Survey. , 1–20.

Wang, Q., Michau, G., & Fink, O. (2020). Missing-class-robust domain adaptation by unilateral alignment for fault diagnosis. *arXiv*. doi: 10.1109/TIE.2019.2962438

Xu, L., Yuan, S., Chen, J., & Ren, Y. (2019). Guided wave-convolutional neural network based fatigue crack diagnosis of aircraft structures. *Sensors (Switzerland)*, *19*(16). doi: 10.3390/s19163567